Science of Sintering, **49** (2018) 15-28

doi: https://doi.org/10.2298/SOS1801015G

UDK 546.831; 621.926.087; 622.785

Dense Zircon ($ZrSiO_4$) Ceramics by a Simple Milling-Sintering Route

Matías R. Gauna[1*)], María S. Conconi[1], Gustavo Suarez[1,2], Esteban Aglietti[1,2], Nicolás M. Rendtorff[1,2]

[1]CETMIC, Centro de Tecnología de Recursos Minerales y Cerámica. Camino Centenario y 506, C.C. 49, (B1897ZCA), M.B. Gonnet, Buenos Aires, Argentina.

[2]Depto. de Química, Facultad de Ciencias Exactas, Universidad Nacional de La Plata, 47 y 115, La Plata, Buenos Aires, Argentina.

Abstract:

In this work, a simple milling sintering route (pressure less) to process dense zircon ceramics from fine (D_{50} 0.8 μm) zircon powders is explored. Particularly, the milling time effect (0-120 min) and the maximum sintering temperature (1400-1600 °C) were studied. The sintering grade developed microstructure and Vickers hardness (Hv) were evaluated and correlated. The dissociation of silicate into (monoclinic and tetragonal) zirconia and silica was evaluated by X-ray diffraction followed by the Rietveld method; it was found to be below 10 wt% in all the studied ranges.

The sintering was enhanced by the milling pretreatment. No sintering additives were incorporated. Dense zircon (porosity below 1 %) ceramics were obtained by a simple milling-sintering route of this high refractory powder at 100-200 °C below the sintering temperature used with conventional processing routes to obtain equivalent final properties. The Vickers hardness reached: 9.0 GPa.

Keywords: *Zircon; Processing; Milling; Sintering; XRD-Rietveld.*

1. Introduction

Zircon ($ZrSiO_4$) refractory materials have a wide range of high temperature and nuclear applications. They exhibit moderately low thermal linear expansion (4×10^{-6} °C^{-1}) and very high chemical inertness even in contact with glassy phase and molten slag. Zircon materials are employed mainly due to their adequate refractoriness, mechanical strength and chemical durability with high-temperature resistance. They have various applications [1-9]. Particularly, it is well known that high refractoriness of zircon ceramics up to high temperatures with attractive properties such as low thermal conductivity, low thermal expansion, chemical stability, and corrosion resistance. These materials also have a moderate resistance to sudden temperature gradients, for example, thermal shock [10-16].

Zircon materials are widely used in glass and steel industries [1, 17-18], especially because pure zircon undergoes no major structural changes below 1680 °C, a temperature at which it dissociates into silica and zirconia. This decomposition temperature decreases with the presence of impurities or mechanical treatments. Zircon materials have structural applications because it has been demonstrated that high purity zircon can retain its bending strength up to temperatures as high as 1200-1400 °C. The corrosion resistance of these

*) **Corresponding author:** matiasrgauna@cetmic.unlp.edu.ar

materials is especially high for glasses with a low amount of alkalis [1, 17-18].

Due to their high refractoriness, zircon powders are difficult to sinter. To overcome this drawback, some additives are usually employed as sintering aids; the typical additives include refractory clays and titanium oxide [19]. But sometimes, this incorporation results in the loss of some of their distinctive properties. Dense zircon ceramics without additives were only processed by advance sintering techniques such as hot pressing [20-21] and SPS [22-24].

It has been reported and proven that the mechanochemical activation in high energy ball milling consists of a suitable pretreatment of raw materials to obtain dense ceramics. Its effect is to activate the chemical and physical processes by incorporating surface energy powders that are usually nanosized, thus effectively achieving homogeneous mixtures of powders even of different sizes [25-29]. Sintering is one of these activated processes.

In a recent article, we reported the effect of colloidal processing optimization by slip casting of highly concentrated aqueous dispersions on the sintering of dense zircon ceramics [30]. In particular, the mechanical behavior of this kind of material is of technological interest and is related to the microstructure, phase composition, and sintering grade. Moreover, the mechanical properties of dense zircon ceramics were reviewed and compared in a recent article [22]. In that article, the effect of milling was also assessed but for a nonconventional advance sintering method (SPS). The effect of Zircon mechanical activation has been a strategy for enhancing zirconia leaching [31]. In this work, the activation for enhancing zircon powder sintering is investigated. The first attempt to study the mechanical activation of zircon was reported by Motoi [32]. It was demonstrated that prolonged ball milling not only causes size reduction but also amorphizes the mineral, which leads to partial decomposition into ZrO_2 and SiO_2 and can also enhance solubility in HF. Puclin and Kaczmarek [33] studied the crystallization of amorphized zircon using a ball mill in which the impact and shear forces can be manipulated. The same group observed that 170-300 h of ball milling of a zircon and alumina mixture resulted in the enhanced dissolution of zircon in hydrochloric acid, which was selective to silica [34]. Similarly, Welham used ball milling up to 150 h to accomplish the mechanochemical reaction of zircon with alkaline earth metal oxides with the objective of forming zirconia or zirconates, either with the milling process or during subsequent annealing at 1200 °C [35-36]. For example, for zirconia (ZrO_2) production from zircon acid leaching, the milling pretreatment process was found to be suitable for enhancing the solubility. In particular, an about tenfold increase in hydrochloric acid solubility was observed when zircon was milled alone and milled with the oxides. Abdel-Rehim showed that almost complete recovery of zirconium from zircon was possible by simultaneous ball milling and alkaline leaching using sodium hydroxide (1.5 times the theoretical requirement) at 250 °C for 3 h [37]. Attrition milling of zircon was used by Amer as a pretreatment to enhance the alkaline pressure leaching of zircon [38]; however, no attempt was made to characterize the activated solid except for the change in particle size. Recently, the zircon milling effect on the zircon alumina reaction sintering to obtain mullite zirconia refractory composites was also proposed and studied. In all these examples, the merits of the strategy were established [39-40].

The aim of this work is to study the effect of high energy ball milling on the sintering behavior of fine zircon powder and characterize the resulting ceramic materials in order to study the possibility of using the milling-sintering strategy to process dense zircon ceramics with good technological properties.

2. Experimental procedure

A commercial zircon powder (Kreutzonit Super Extra Weiß, Mahlwerke Helmut Kreutz GmbH, Germany, 0.8 μm) was used (Z0). High energy ball milling (HEBM) in a planetary mill (7 Premium Line, Fritsch Co., Ltd., Germany) at 850 rpm was performed for 10, 60 and 120 min (Z10, Z60, and Z120, respectively). The employed jar and milling media

were made of zirconia; 85 ml zirconia jars were used with 60 g of zirconia balls (10 mm diameter) as milling media; the ratio between the weight of powder and the milling balls was 1:10 in each batch. The jars were cooled down every 5 min.

The effect of the milling treatment was characterized by measuring the particle size distribution with a Laser Diffraction Particle Size Distribution Analyzer (Malvern Hydro 2000G). The percentile population on a logarithmic scale below 90, 50 and 10 were calculated (D90, D50, and D10 respectively).

The particle shape and morphology were also analyzed with scanning electron microscopy (SEM-JEOL JMS -6000, Japan), and X-ray diffraction (XRD-Philips PW 3710 with Kα: Cu as incident radiation and Ni filter) was performed at 2θ between 10 and 70° to evaluate the effect of the milling time. Rietveld refinement was performed in order to follow the partial zircon dissociation [41-43].

Disc-shaped samples of 15 mm diameter were prepared; they were first uniaxially pressed in a steel mold and then isostatically pressed at 1000 MPa in an oil bath. Samples were then sintered at 1400, 1500 and 1600 °C in an electric furnace. The employed heating rate was 5 °C/min in all cases, with a holding time of 2 hours at a cooling rate of 5 °C/min.

Sintered samples were characterized measuring the textural properties of the Archimedes method. The evolution of the crystalline composition with the sintering temperature was evaluated by X-ray diffraction and Rietveld refinement [41-43]. The developed microstructures were evaluated by scanning electron microscopy (SEM-JEOL JMS-6000, Japan). Finally, in order to assess the mechanical properties of the developed materials, the Vickers hardness was evaluated (Buhhler, USA). 3 Kg load and 15-second dwelling were employed for the hardness experiments. These characterizations were correlated with the processing variables: milling time and final sintering temperature.

3. Results and Discussion

3.1. Effect of the milling process, particle size distribution for laser scattering

The particle size distribution analysis was performed for the original (Z0) and the milled samples at 10, 60 and 120 min (Z10, Z60, and Z120, respectively) in order to observe the particle size evolution. Table I lists the results of the particle size analysis. The observed effect of the milling treatment is negligible. The mean particle size remained constant even after 120 min of pretreatment.

Tab. I Particle size distribution of the milled powders.

Sample	Milling time (min)	d_{10} (µm)	d_{50} (µm)	d_{90} (µm)
Z0	0	0.5	1.1	2.6
Z10	10	0.5	1.1	2.4
Z60	60	0.5	1.1	2.7
Z120	120	0.4	1.1	2.8

3.2. Effect of the milling process, scanning electron microscopy (SEM)

Fig. 1 (a, b, c and d) show SEM images of the Z0 and Z120 samples at two magnifications (10000x and 30000x). Fig. 1a–c depicts the SEM image of the as-received zircon powder, showing sharp edges and grain sizes between 2 μm and 0.1 μm. Fig. 1b–d shows the powder after 120 min of HEBM. After the milling process, the particles were more rounded, but no significant change in the particle size was detected, as confirmed by laser diffraction. No important agglomeration was observed.

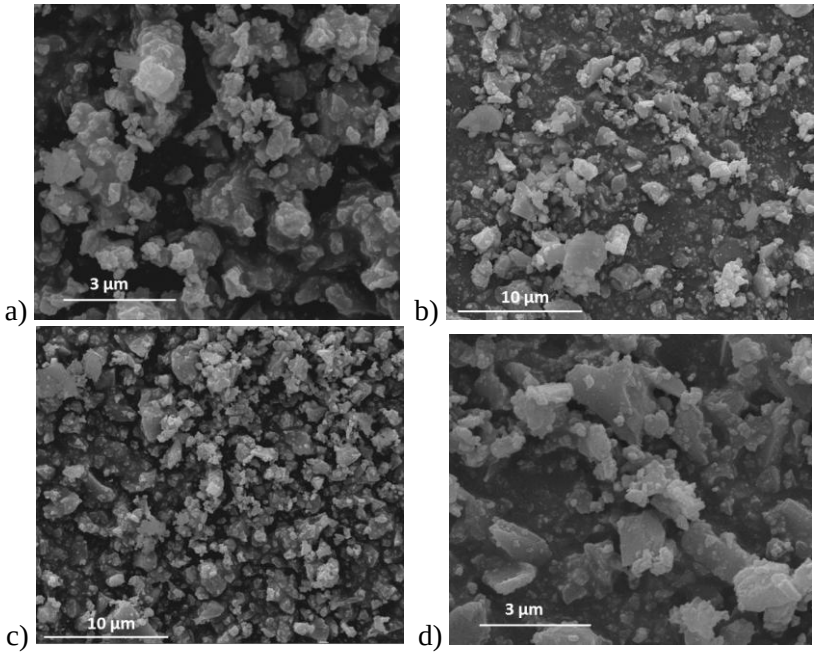

Fig. 1. SEM images of the as-received and milled powders: a) Z0, 10000X; b) Z120, 10000X; c) Z0, 30000X; and d) Z120, 30000X.

3.3. Effect of the milling pretreatment on the crystalline zircon phase by X-ray diffraction

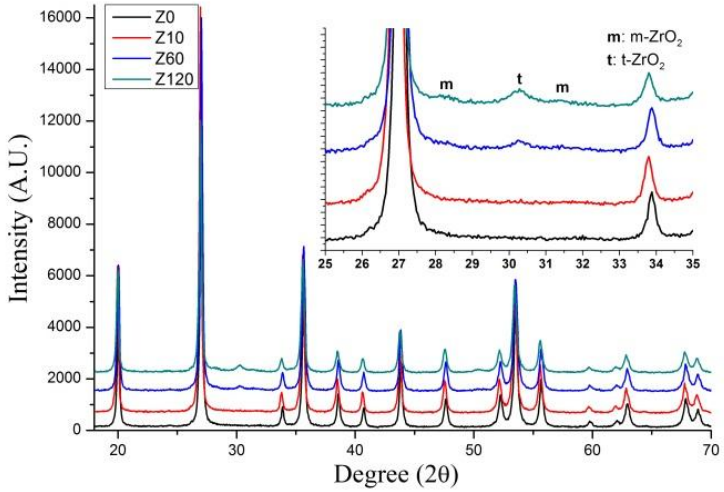

Fig. 2. XRD patterns of the milled and unmilled fine zircon powders.

The HEBM pretreatment might lead to partial zircon dissociation [8-9]:

$$ZrSiO_4 \leftrightarrow \text{(m-t) } ZrO_2 + SiO_2 \text{ (amorphous)} \quad (1)$$

Fig. 2 compares the XRD patterns of the powder before and after the HEBM. Regardless of the milling time, all the observed diffraction peaks belong to the zircon phase. No important broadening of the peaks is observed, showing that the pretreatment did not affect the zircon crystallinity. This is expected due to the high hardness of the silicate (7.5 in the Mohs scale). The inset in this Fig. shows the main peaks of the zirconia phases (m and t/c) in the 2θ range. Only after 60 min of pretreatment does a small band appear at 30.3°, which corresponds to the high energy (tetragonal and/or cubic) zirconia phases [44]. After the 120-minute treatment, this peak is bigger but still small. It is accompanied by the main monoclinic (lower energy) zirconia peaks located at 28.3° and 31.5°, corresponding to the (-111) and (111) planes. All this was clear evidence of the incipient silicate dissociation.

3.4. Sintering of milled powders

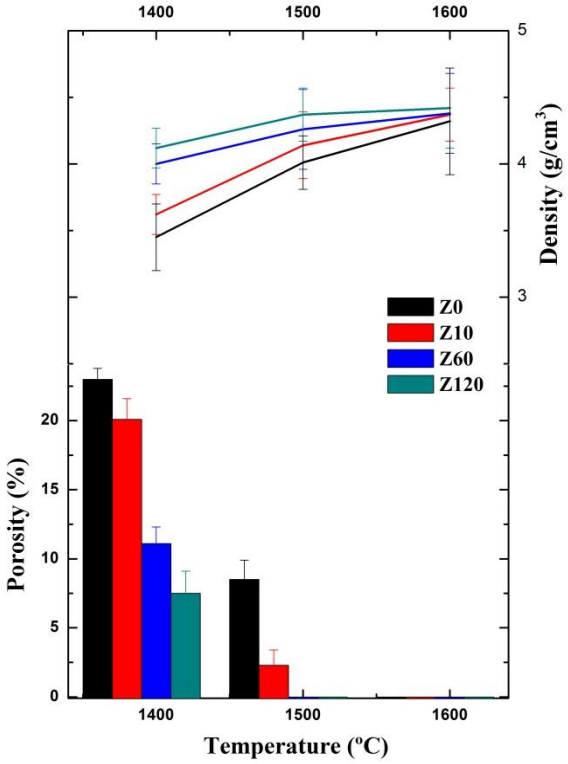

Fig. 3. Textural properties, density and porosity of the milled-sintered powders. Samples Z0, Z10, Z60 and Z120 sintered at 1400, 1500 and 1600 °C.

Fig. 3 shows the evolution of the textural properties. As expected, while density increases with the sintering temperature, the open porosity decreases. The untreated powder had a high porosity (23 %) at 1400 °C, and achieved full densification at 1600 °C.
Remarkably, materials sintered at 1500 °C were fully densified if the pretreatment consisted of 60 and 120 minute milling. At that temperature, the 10-minute treated sample had a low porosity (3 %). For several applications, this low porosity could be understood as a dense material [2]. However, important differences were observed in the materials sintered at 1400 and 1500 °C. At 1400 °C, the sintering of the milled powders was directly proportional to the

milling time. The 10-minute milled powder porosity was 19 %. The 120 minute milled powder porosity was below 10 %, evidencing the effect of the mechanical treatment.

The sintering achieved was high in comparison with previous work using coarser zircon powder (2-5 μm) grains processed by slip casting [17]. At the highest temperature, the four powders sintered completely.

The fully dense ceramic obtained without sintering additives by HEMB, followed by conventional sintering, represents an achievement in the processing of zircon ceramic. In fact, by employing conventional sintering methods, fully dense zircon cannot be obtained at a temperature as low as 1400 °C [17]. Shi et al. [20] obtained fully dense zircon material by hot pressing at 1600 °C for 1 h under 25 MPa. A 5% residual open porosity was achieved without full densification by pressureless sintering of slip casted materials [30].

3.5. Crystalline phases of the obtained ceramics

The final crystalline phase combination in this kind of refractory material is a very important factor for the technological properties. It will define the corrosion, mechanical and thermomechanical behaviors [45-47]. For example, the formed zirconia might be involved in several toughening mechanisms [44, 48-49] and can improve the molten glass corrosion resistances [50]. On the other hand, the silica-based glassy phase might enhance sintering by viscous flux and may have a deleterious effect on the mechanical behavior of the material, especially at high temperatures [1, 8].

The partial dissociation of zircon materials during thermal processing has been previously reported [8]. The grade of dissociation will simultaneously depend on the impurities, particle size, and presumably will be affected by the milling pretreatment. Kaiser et al. presented an extensive review on this issue [8]. While the dissociation will thermodynamically start near 1680 °C, in the presence of impurities it can be lowered by around two hundred degrees [51-52].

The already decomposed zircon reassociates at 1278–1556 °C with a maximum reaction rate above 1444 °C. Zircon formation starting from ZrO_2 and quartz, cristobalite, tridymite or amorphous silica did not show any significant dependence on the starting silica modifications. The lowest formation temperature observed was 1333 °C, which is only a little higher than the lowest temperature of reassociation reported, i.e., 1278 °C [8]. This explains the reversible arrows in Eq. 1.

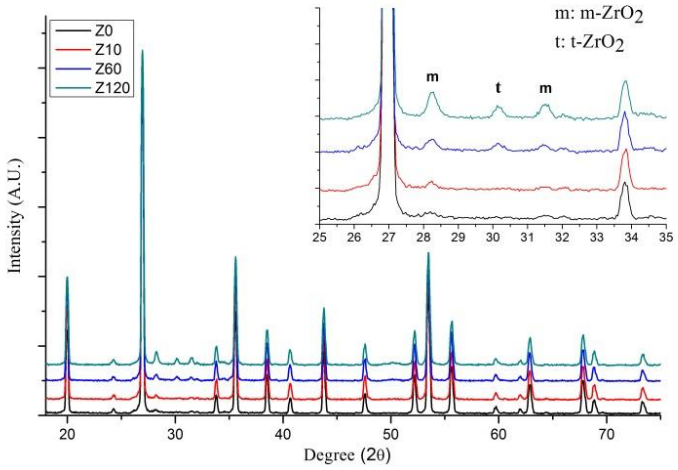

Fig. 4. XRD patterns of sintered materials at 1400 °C processed from milled powders with 0, 10, 60 and 120 minute milling treatments.

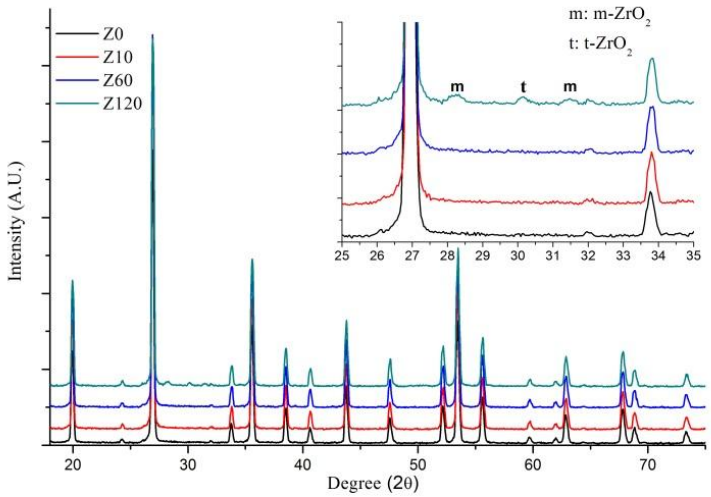

Fig. 5. XRD patterns of sintered materials at 1500 °C processed from milled powders with 0, 10, 60 and 120 minute milling treatments.

The final crystalline compositions of the developed materials were evaluated by X-ray diffraction. Fig.s 4, 5 and 6 show XRD patterns of materials obtained by different milling-sintering programs, particularly sintered at 1400, 1500 and 1600 °C, respectively. Then, the four powders were evaluated at each temperature (0, 10, 60 and 120 min). In all cases, the major crystalline phase is the zirconium silicate. Zircon peaks are accompanied by the main peaks of both the monoclinic and the high energy tetragonal or cubic phases. The detail for the 26-35° 2θ range is plotted as an inset in the three Fig.s.

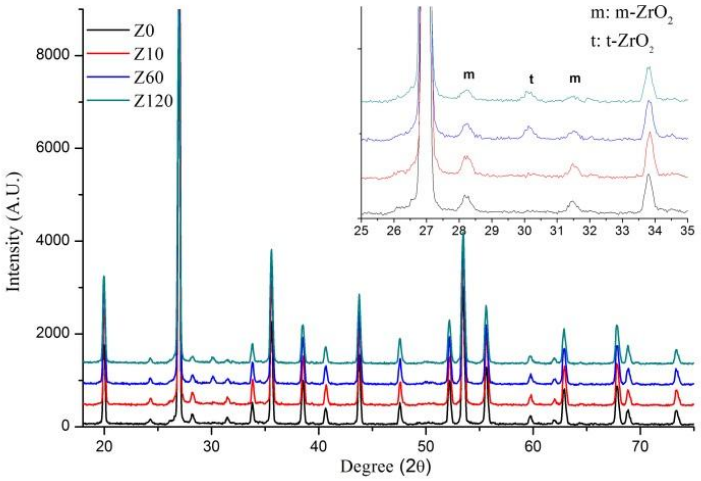

Fig. 6. XRD patterns of sintered materials at 1600 °C processed from milled powders with 0, 10, 60 and 120 minute milling treatments.

The Rietveld refinement allowed us to quantify the crystalline phases (zircon and zirconia). Once again, no silica phases (quartz, cristobalite or tridymite) were detected. The results of the Rietveld quantification are listed in Table 2; the resulting values of the Rwp parameters were in all cases adequate and below 15.

Tab. II Results of the Rietveld method phase quantification of the milled-sintered samples.

Sample	Milling Time (min)	Sintering temp. (°C)	Crystalline phase content (wt%) Error between brackets		
			$ZrSiO_4$	m-ZrO_2	t-ZrO_2
Z0-1400	0	1400	100	0	0
Z0-1500	0	1500	98 (0.5)	2 (0.1)	0
Z0-1600	0	1600	94 (0.8)	6 (0.3)	0
Z10-1400	10	1400	100 (0)	0	0
Z10-1500	10	1500	98 (0.4)	2 (0.1)	0
Z10-1600	10	1600	94 (0.6)	6 (0.2)	0
Z60-1400	60	1400	100 (0)	0	0
Z60-1500	60	1500	95 (0.4)	4 (0.1)	1 (0.1)
Z60-1600	60	1600	94 (0.4)	4 (0.1)	2 (0.1)
Z120-1400	120	1400	96 (0.4)	3 (0.1)	1 (0.1)
Z120-1500	120	1500	90 (0.4)	8 (0.2)	2 (0.1)
Z120-1600	120	1600	95 (0.4)	3 (0.2)	1 (0.1)

In the studied ranges, in terms of sintering temperature and pretreatment time, the dissociation was below 10 % in all cases. Some particular aspects can be pointed out.
The untreated powder showed no dissociation after 1400 °C and an incipient dissociation after 1500 °C. At 1600 °C, this dissociation was over 6 wt%. In both cases, the resulting zirconia phase was the low (energy) monoclinic zirconia.

Another relevant aspect is that after the 1400 °C thermal treatment, the dissociation occurred only for the 120 minute milled powder. No zirconia was detected in the other materials.

In general, a direct relation between the two explored processing variables would be expected. Both the milling pretreatment and maximum sintering temperature will enhance sintering and silicate dissociation this was confirmed in the whole studied range. Z120 powder sintered at 1600 °C (Z120-1600) was an exception. The more dissociated processed material was the Z120-1500 material, which achieved 10 % silicate dissociation. The decrease in the resultant dissociation of the Z120-1600 material might be explained in terms of the reassociation of the important amount of amorphous silica and zirconia, previously dissociated during the mechanical pretreatment, detected by XRD (see inset in Fig. 2) [8].

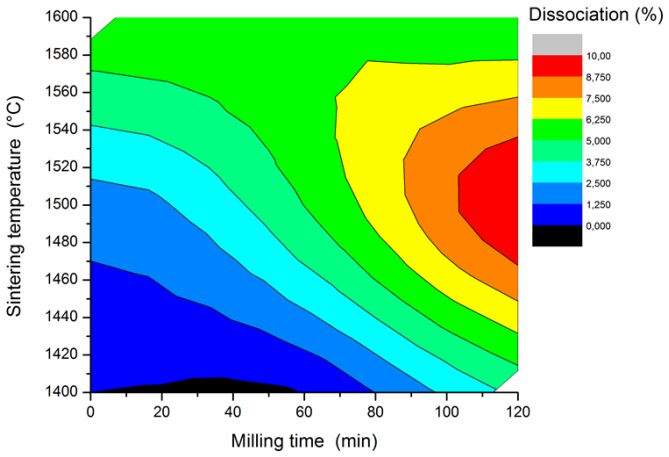

Fig. 7. Contour plot of the sintering temperature-milling time effect on the zircon dissociation of the developed materials. The zircon dissociation (%) was assumed to be $ZrO_2/ZrSiO_4$.

With the XRD-Rietveld quantification of the systematically explored processing variables, a contour plot was constructed (Fig. 7) by interpolation. As dissociation parameter, the total zirconia:zircon percentile ratio was plotted as a function of the sintering temperature and the milling time. Again, the effects of both processing variables are clearly observed; they both enhance the dissociation, but the excessive milling (≈120 min) restricts the thermal dissociation.

3.6. Microstructure of the obtained zircon ceramics

The microstructures developed were evaluated by scanning electron microscopy. SEM images of the partially and fully sintered materials are presented in Fig.s 8 and 9, respectively. Apparently, the conforming route (pressing) was adequate, no macropores were observed. A homogeneous microstructure was obtained in all the materials.

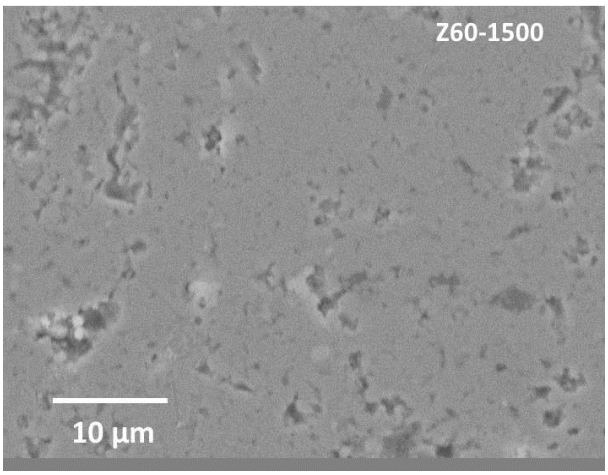

Fig. 8. SEM image of the Z60-1500 material sintered at 1500 °C and milled for 60 min.

Fig. 8 shows the untreated powder sintered at 1400 °C (Z0-1400); the porosity evaluated by the Archimedes method (P) is observed. The neck formation bonding the zircon grains (Zn) indicates that the sintering process is in its initial stage in some cases [53, 55]. The observed pore size (in dark gray) corresponds to the initial grain size (0.8 µm). As evaluated by XRD, no white zirconia grains are observed.

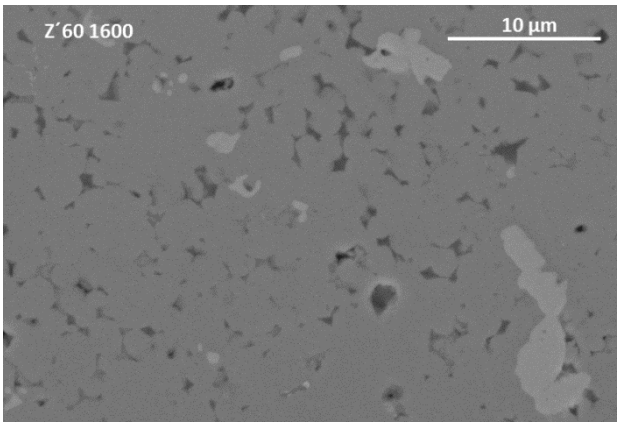

Fig. 9. SEM image of the Z60-1600 material sintered at 1600 °C and milled for 60 min.

On the other hand, a fully dense ceramic material (Z0-1600) is depicted in Fig. 9. In this case, the sintering process is advanced, only some small pores are observed (P), the pore size is smaller than in Fig. 8. In some cases, grain sizes are slightly higher than in the initial powder. Other grains are evidently larger, with diameters between 5 and 8 μm, which evidence some local sintering. Zircon grains (Zn) are accompanied by zirconia grains (Z: white), and glassy grain boundaries can also be seen (G). This microstructure is similar to the one observed in this same material but obtained through different processing routes (hot pressing, SPS, slip casting, etc.) [2, 8, 13, 16, 19, 20, 22, 30]. This kind of microstructure, where the zirconia grains are imbibed in a dense ceramic microstructure, has been widely studied. Several reinforcement mechanisms have been proposed and observed in this kind of system [44, 49].

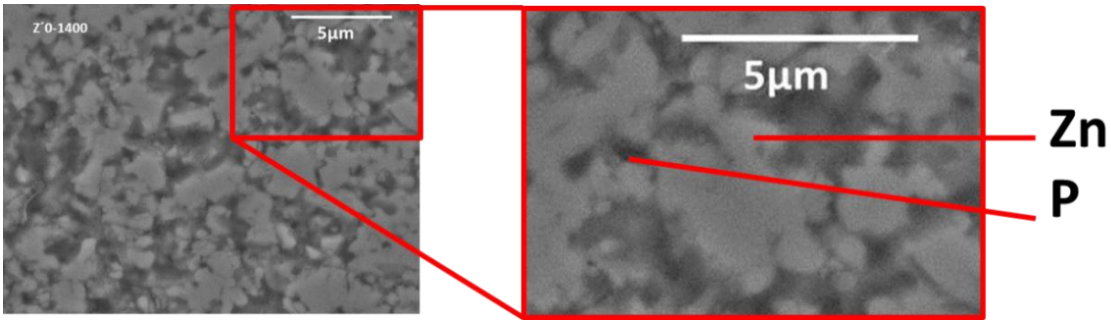

Fig. 10. SEM image and digitally enlarged SEM image of the partially sintered Z01400 material at 1400 °C. (P: Pore, Zn: $ZrSiO_4$).

Fig.s 10 and 11 present the microstructure of the materials based on the 60-minute milled powder (Z60) sintered at 1500 and 1600 °C (Z60-1500 and Z60-1600). In general, the obtained microstructures are similar to the one shown in Fig. 9. Dense zircon materials with the presence of some pores and some imbibed zirconia grains can be observed. This fact is a merit of the processing route. An identical or equivalent microstructure can be obtained even at lower temperatures (reduced by about ≈ 200 °C).

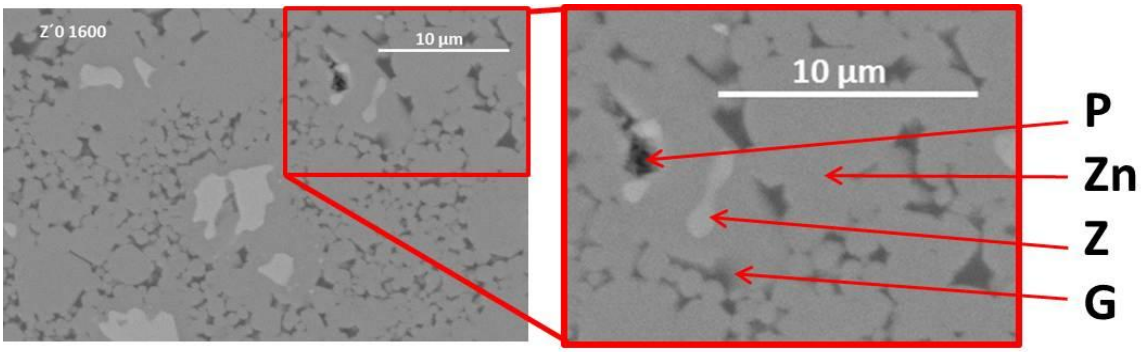

Fig. 11. SEM image and digitally enlarged SEM image of the fully sintered Z0-1600 material at 1600 °C. (P: Pore, Zn: $ZrSiO_4$, Z: ZrO_2, G: glassy SiO_2 phase).

3.7. Mechanical behavior of the developed ceramics

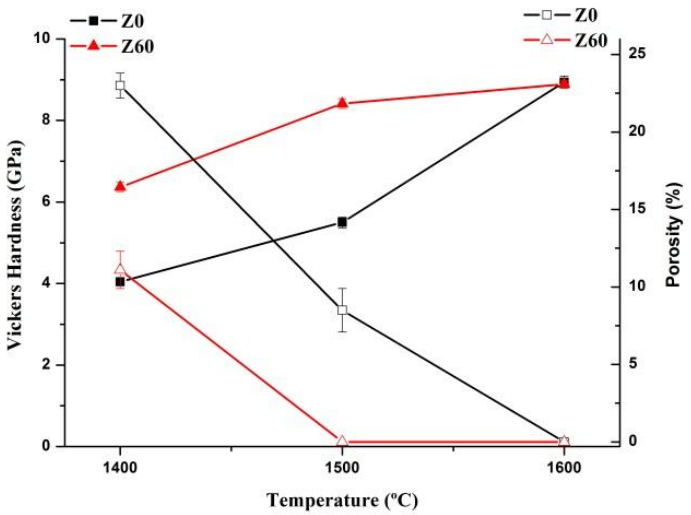

Fig. 12. Vickers hardness (Hv) and porosity (P) of the unmilled (Z0) and milled (Z60) sintered at 1400, 1500 and 1600°C.

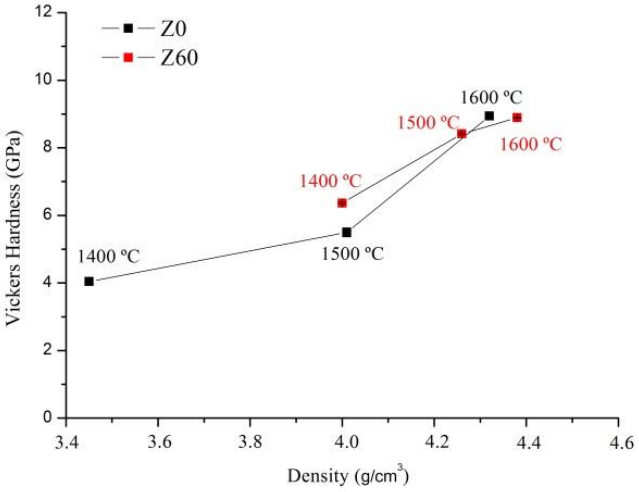

Fig. 13. Vickers hardness (Hv) as a function of density for unmilled (Z0) and 60-minute milled (Z60) materials sintered at 1400, 1500 and 1600 °C.

The Vickers hardness (Hv) and open porosity (%) of the unmilled (Z0) and 60-minute milled (Z60) powders as a function of the sintering temperature are plotted in Fig. 12. Also, Hv as a function of the final density is plotted in Fig. 13. Evidently, the achieved Hv was directly related to the sintering temperature, and clearly the milling treatment time enhanced sintering, so the mechanical behavior improved. The approximately 9.0 GPa Hv achieved is similar to that of other dense zircon ceramics [21-24]. Finally, it can be noted that the hardness of Z0-1600 is similar (between 8.0 and 9.0 GPa) to the one of Z60-1500 and Z60-1600. It can be stated that the Hv at high temperatures is independent of the processing route, but the final sintering temperature can be reduced by at least 100 °C.

4. Conclusions

A simple processing route based on different milling-sintering times for obtaining dense zircon ceramics from fine zircon powders was proposed and systematically studied. Within the milling time (0-120 min) and sintering temperature (1400-1600 °C) ranges studied, the milling pretreatment led to partial dissociation of the starting zircon powders into zirconia and silica (below 10 wt%). No important effect on the particle size distribution was found after milling. A slight effect on the grain morphology was observed and described after the SEM evaluation of the milled powders. The most significant effect of the milling pretreatment was the sintering activation, which is remarkable taking into account the high zircon hardness and refractoriness.

Without the incorporation of sintering additives, dense zircon ceramics (porosity below 1%) were obtained by a simple milling-sintering route of this high refractory powder at 100-200 °C below the sintering temperature used with conventional processing routes for obtaining equivalent final properties. The Vickers hardness reached 9.0 GPa.

5. References

1. I. G. Mel'nikova, T.A. Nesterova, I.V. Razdol'skaya, Glass Ceram+, 42 (1985) 295.
2. X. Carbonneau, M. Hamidouche, C. Olagnon, G. Fantozzi, R. Torrecillas, Key Eng. Mat., 132-136 (1997) 571.
3. P. Tartaj, C. J. Serna, J. S. Moya, J. Requena, M. Ocana, S. De Aza, F. Guitian, J. Mater. Sci., 31 (1996) 6089.
4. C. Abajo, A. Jiménez-Morales, J. M. Torralba, Bol. Soc. Esp. Ceram. V., 54 (2015) 93.
5. T. Mori, H. Yamamura, H. Kobayashi, T. Mitamura, J. Am. Ceram. Soc., 75 (1992) 2420.
6. Y. Ding, X. Lu, H. Dan, X. Shu, S. Zhang, T. Duan, Ceram. Int., 41 (2015) 10044.
7. L. B. Garrido, E. F. Aglietti, Ceram. Int., 27 (2001) 491.
8. A. Kaiser, M. Lobert, R. Telle, J. Eur. Ceram. Soc., 28 (2008) 2199.
9. C. E. Curtis, H. G. Sowman, J. Am. Ceram. Soc., 36 (1953) 190.
10. F. Ya. Kharitonov, O. A. Sheronova, A. E. Volokhov, G. F. Dobrynin, Glass Ceram+ (English translation of Steklo i Keramika), 45 (1989) 266.
11. T. Ebadzadeh, Adv. Appl. Ceram., 108 (2009) 381.
12. M. Hamidouche, N. Bouaouadja, R. Torrecillas, G. Fantozzi, Ceram. Int, 33 (2007) 655.
13. N. M. Rendtorff, L. B. Garrido, E. F. Aglietti, Mater. Sci. Eng. A, 498 (2008) 208.
14. N. M. Rendtorff, L. B. Garrido, E. F. Aglietti, Ceram. Int., 35 (2009) 779.
15. N. M. Rendtorff, E. F. Aglietti, Mater. Sci. Eng. A., 527 (2010) 3840.
16. N. M. Rendtorff, G. Suárez, Y. Bruni, L. B. Garrido, E. F. Aglietti, Adv. Sci. Tech., 70 (2010) 59.
17. N. M. Rendtorff, L. B. Garrido, E. F. Aglietti, Ceram. Int., 37 (2011) 1427.
18. K. Kato, N. Araki, J. Non-Cryst. Solids, 80 (1986) 681.
19. M. Awaad, S. H. Kenawy, Brit. Ceram. T., 102 (2003) 69.
20. Y. Shi, X. Huang, M. Ruan, D. Yan, Mater. Lett., 23 (1995) 247.
21. S. Huang, Q. Li, Z. Wang, X. Cheng, H. Wen, Ceram. Int., 43 (2017) 875.
22. N. M. Rendtorff, S. Grasso, C. Hu, G. Suarez, E. F. Aglietti, Y. Sakka, Ceram. Int., 38 (2012) 1793.
23. N. M. Rendtorff, S. Grasso, C. Hu, G. Suarez, E. F. Aglietti, Y. Sakka, J. Eur. Ceram. Soc., 32 (2012) 787.

24. M. C. Anjali, P. Biswas, D. Chakravarty, U. S. Hareesh, Y. S. Rao, R. Johnson, Sci. of Sint., 44 (2012) 323.
25. C. Suryanarayana, Prog. Mater. Sci., 46 (2001) 1.
26. B. S. Murty, S. Ranganathan, Int. Mater. Rev., 43 (1998) 101.
27. W. S. Jung, H. S. Park, Y. J. Kang, D.H. Yoon, Ceram. Int., 36 (2010) 371.
28. J. Yang, T. Zhang, K. Cui, Z. Hu, Act. Metall. Sin.-Chin. Ed., 33 (1997) 3859.
29. C. Duran, K. Sato, Y. Hotta, T. Nagaoka, K. Watari, J. Ceram. Soc. Jpn., 116 (2008) 1175.
30. G. Suárez, S. Acevedo, N. M. Rendtorff, L. B. Garrido, E. F. Aglietti, Ceram. Int., 41 (2015) 1015.
31. S. Srikanth, V. L. Devi, R. Kumar, Hydrometallurgy, 157 (2015) 159.
32. S. Motoi, J. Ceram. Assoc. Jpn,. 86 (1978) 92.
33. T. Puclin, W. A. Kaczmarek, Colloid Surface A., 129 (1997) 365.
34. T. Puclin, W. A. Kaczmarek, B. W. Ninham, Mater. Chemistry Phys., 40 (1995) 105.
35. N. J. Welham, Metall. Mater. Trans. B., 29 (1998) 603.
36. N. J. Welham, J. Am. Ceram. Soc., 85 (2002) 2217.
37. A. M. Abdel-Rehim, Int. J. Miner. Process, 76 (2005) 234.
38. M. A. Ashraf, Physicochem. Probl. Mi., 40 (2006) 61.
39. S. Ghaffari, M. Alizadeh, K. Asadian, T. Ebadzadeh, A. Ghanbari, IET Micro Nano Letters, 8 (2013) 193.
40. R. Emadi, H. Ashrafi, R.Zamani Foroushani, Ceram. Int., 41 (2015) 14400.
41. H. M. Rietveld, Journal of Applied Crystallography, 2 (1969) 65.
42. D. L. Bish, J. E. Post, Am. Mineral., 78 (1993) 932.
43. M. R. Gauna, M. S. Conconi, S. Gomez, G. Suarez, E. F. Aglietti, N. M. Rendtorff, Ceram-Silikaty, 50 (2015) 318.
44. X. Jin, Curr. Opin. Solid State Mater. Sci., 9 (2005) 313.
45. W. E. Lee, R. E. Moore, J. Am. Ceram. Soc., 81 (1998) 1385.
46. C. Sadik, I. E. El Amrani, A. Albizane, J. Asian Ceram. Soc., 2 (2014) 83.
47. A. Mukhopadhyay, B. Basu, Int. Mater. Rev., 52 (2013) 257.
48. R. HJ Hannink, P. M. Kelly, B. C. Muddle, J. Am. Ceram. Soc., 83 (2000) 461.
49. N.M. Rendtorff, L.B. Garrido, E.F. Aglietti, Ceram. Int., 36 (2010) 781.
50. M. F. Zawrah, Ceram. Int., 33 (2007) 751.
51. P. Pena, S. De Aza, J. Mater. Sci., 19 (1984) 135.
52. N. M. Rendtorff, S. Gómez, M. R. Gauna, M. S. Conconi, G. Suarez, E. F. Aglietti, Ceram. Int., 42 (2016) 1563.
53. R. Chaim, M. Levin, A. Shlayer, C. Estournes, Adv. Appl. Ceram., 107 (2008) 159.
54. K. Lu, Int. Mater. Rev., 53 (2008) 21.
55. H. Belhouchet, H. Makri, M. Hamidouche, M. Bouaouadja, V. Garnier, G. Fantozzi, Sci. of Sint., 46 (2014) 291.

Садржај: *У овом раду, једноставан метод млевења и синтеровања је коришћен за добијање густе цирконијумске керамике из финог ситног праха (D_{50} 0.8 μm). Заправо, проучавани су утицај времена активације (0-120 мин) и максимум температуре синтеровања (1400-1600 °C). Стадијум синтеровања, микроструктура и тврдоћа по Викерсу су проучавани. Дисоцијација силиката у цирконијуму и силикат су одређени рендгено структурном анализом и Ритвелдовим утачњавањем; нађено је да је дисоцијација мања од 10 тежинских % у свим узорцима. Синтеровање је поспешено претходном механичком активацијом. Нису употребљавани адитиви. Густа цирконијумска керамика (порозности испод 1 %) је добијена једноставним млевење-синтеровање поступком на температурама мањим за 100-200 °C од температура*

синтеровања које су потребне за добијање керамике без претходног третмана. Тврдоћа по Викерсу је 9.0 GPa.
Кључне речи: *цирконијум; процесирање; млевење; синтеровање; Ритвелд.*